

Preparation and Characterization of Fe-Tetranitro Phthalocyanine/Polyurethane Blends

Yang Ti, Dajun Chen

State Key Laboratory for Modification of Chemical Fibers and Polymer Materials,
College of Materials Science and Engineering, Donghua University, Shanghai 201620, China
Correspondence to: D. Chen (E-mail: cdj@dhu.edu.cn)

ABSTRACT: In this article, Fe-Tetranitro phthalocyanine (Fe-TNPc)/polyurethane (PU) blends were prepared by solution blending. The mechanical properties of the samples were studied by tensile tests. The results showed that the tensile strength and the elongation at break of the samples increased with increasing Fe-TNPc content. The improved mechanical properties for the samples containing Fe-TNPc was attributed to the increased microphase separation degree of PU, which was further investigated by dynamic mechanical analysis (DMA) and Fourier transform infrared analysis. The lower T_g of the soft segments and the higher T_g of the hard segments for the samples containing Fe-TNPc indicated an increase of microphase separation degree of PU. The increased hydrogen bonded carbonyl groups in the samples with increasing Fe-TNPc content also proved the conclusion. Quantitative evaluation of the interaction between Fe-TNPc and PU was also investigated by analyzing the physical crosslinking density of the samples. The results indicated that the physical crosslinking density of the samples increased with increasing Fe-TNPc content. The antibacterial properties of the samples were investigated. The results showed that the percentage bacterial inactivation toward *S. aureus* and *E. coli* of the samples were 98.9% and 90.9%, respectively, when Fe-TNPc was added to 1%. © 2014 Wiley Periodicals, Inc. *J. Appl. Polym. Sci.* **2015**, *132*, 41284.

KEYWORDS: blends; films; functionalization of polymers, properties, and characterization; polyurethanes

Received 23 April 2014; accepted 11 July 2014

DOI: 10.1002/app.41284

INTRODUCTION

Due to its superior mechanical, flexibility, and abrasive resistance properties, polyurethane (PU) has been widely used in various fields, such as coating, adhesives, fabric, films, and so on.^{1–5} However, the rough topology of PU films (due to its segmental structure) serves as a good anchorage substrate for cells. Thus, bacteria are susceptible to grow on it. The drawback of PU limited its applications in daily life.^{6–8} In order to improve PU's antibacterial properties, the incorporation of antibacterial agents, such as Ag, TiO₂, ZnO, etc., to PU matrix has attracted the most attention.^{9–12} Liu et al.⁹ embedded silver nanoparticles (AgNPs) into a waterborne polyurethane (WPU) matrix. The prepared material had a strong bacteriostatic effect on the growth of *S. aureus* and *E. coli*. They also found that the higher efficiency of bacteria inhibition was obtained in the samples with good dispersion of AgNPs in WPU. Ma et al.¹⁰ Prepared WPU/flower-like ZnO (f-ZnO) nanowhisker composite by *in situ* copolymerization process. The antibacterial activities of WPU against *S. aureus* and *E. coli* were enhanced.

Recently, as a group of promising photosensitizers, phthalocyanine (Pc), and its derivatives were given special attention due to their strong absorption in the visible region of the spectrum, high efficiency in bacterial inactivation, ease of chemical modification and formulation and extraordinary stability.^{13–17} Researchers mainly concerned the antibacterial properties of Pc itself. Only a few studies involved the role of Pc playing in a Pc/polymer blend.^{14,15} Masilela et al.¹⁴ prepared a polystyrene fiber containing low symmetrically substituted Pc by electrospun. They found that the modified polymer fiber showed high antimicrobial activity toward *S. aureus* under illumination with visible light.

In our previous reports, Fe-octacarboxyl acid phthalocyanine (Fe-OCAP)/polyurethane (PU) blends were prepared.^{18–20} Improved antibacterial property of the samples was obtained by the addition of Fe-OCAP. However, Fe-OCAP had a high aggregated tendency due to its strong polar group –COOH. The aggregation would reduce its efficiency in bacterial inactivation.

In this article, a relatively weak polar group, nitro-group, substituted Pc, Fe-Tetranitro Phthalocyanine (Fe-TNPc), was

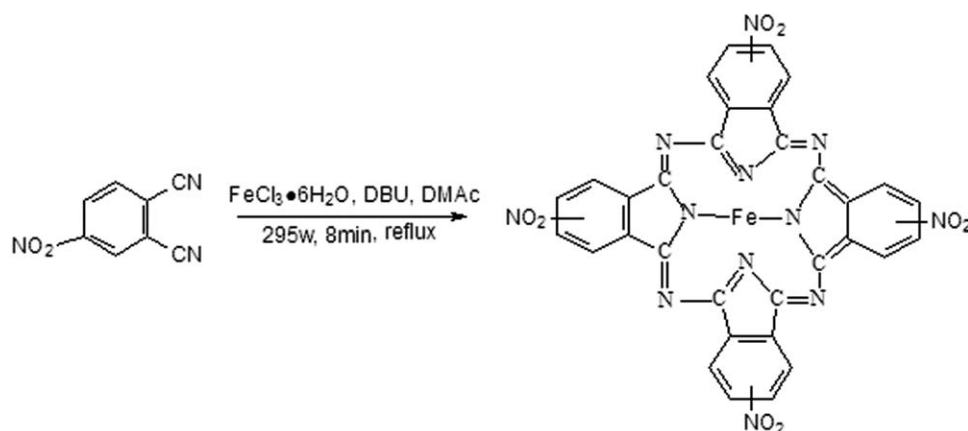
Additional Supporting Information may be found in the online version of this article.

© 2014 Wiley Periodicals, Inc.

Table I. The Experimental Conditions for the Synthesis of Fe-TNPc^a

Catalyst (mL)	0.01	0.1	0.2	0.3	0.4	0.5	0.2	0.2	0.2	0.2	0.2	0.2
Microwave Power (W)	295	295	295	295	295	295	200	220	240	260	280	295

^aThe weight of 4-nitrophthalonitril and FeCl₃·6H₂O were 0.69 g and 0.27 g, respectively. The amount of DMAc was 10 mL. The reacting time was 8 min.

**Scheme 1.** Synthesis of Fe-TNPc.

synthesized. Fe-TNPc/PU blends with different Fe-TNPc content were prepared. The effects of Fe-TNPc content on the mechanical, dynamic mechanical, and antibacterial properties of the blends were studied by tensile tests, dynamic mechanical analysis, and antibacterial tests, respectively. The interaction between Fe-TNPc and PU was investigated by infrared analysis.

EXPERIMENTAL

Materials

FeCl₃·6H₂O was purchased from Sinopharm Chemical Reagent Co., Ltd., China. Dimethylacetamide (DMAc) was purchased from Shanghai Jingwei Chemical Co., Ltd., China. 4-Nitrophthalonitril and 1,8-Diazabicyclo[5.4.0]undec-7-ene (DBU) were purchased from J&K Scientific, China. All the chemicals were of analytical grade. The PU sample (TPU 1180A) was obtained from BASF (commercial). The hard segments were composed of 4,4'-diphenylmethane diisocyanate (MDI) chain extended with butanediol and the soft segments were composed of polytetramethylene ether glycols (PTMEG).

Sample Preparation

Synthesis of Fe-TNPc. Fe-TNPc was synthesized according to references.^{21–24} 4-Nitrophthalonitril (0.69 g, 4.0 mmol) and FeCl₃·6H₂O (0.27 g, 1.0 mmol) were dissolved in DMAc (10 mL) in a flask first. Then DBU, which was used as catalyst, was added in. The mixture was stirred for one minute. Then the reaction mixture was continuously stirred and irradiated in a focused microwave oven (Discover) for 8 min. The amount of catalyst and the irradiation power were determined by our following tests. The product was washed with distilled water to remove DMAc. It was then purified using alcohol and acetone for three times and was dried in a vacuum to get a dark green

powder. The yield of Fe-TNPc was calculated by the following equation.

$$\text{Yield}(\%) = W_3 / (W_1 + W_2) \times 100\%$$

where W_3 is the weight of the final product reacted under different conditions, W_1 is the weight of 4-Nitrophthalonitril, and W_2 is the weight of FeCl₃·6H₂O. The reacting conditions are listed in Table I.

Preparation of Fe-TNPc/PU Films. Fe-TNPc (0.1 g) was dissolved in DMAc (100 g) in a three necked flask first. PU (10 g) were then added into the solution and stirred at 75°C for 6 hours. The blending solutions were then casted on glass plates, and placed in vacuum at 60°C for 3 days to remove the residual

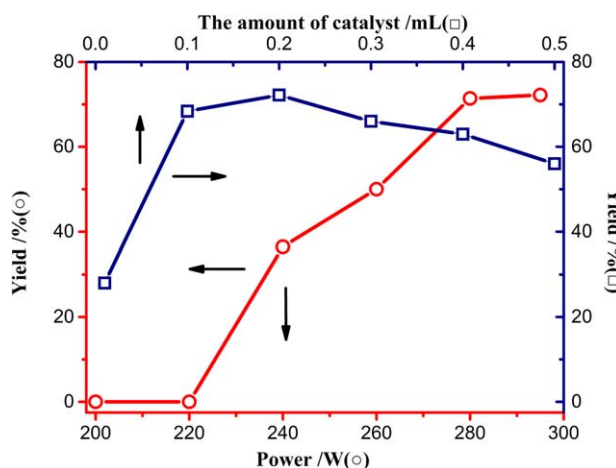


Figure 1. The influence of the microwave power and the amount of catalyst to the yield of Fe-TNPc. [Color figure can be viewed in the online issue, which is available at wileyonlinelibrary.com.]

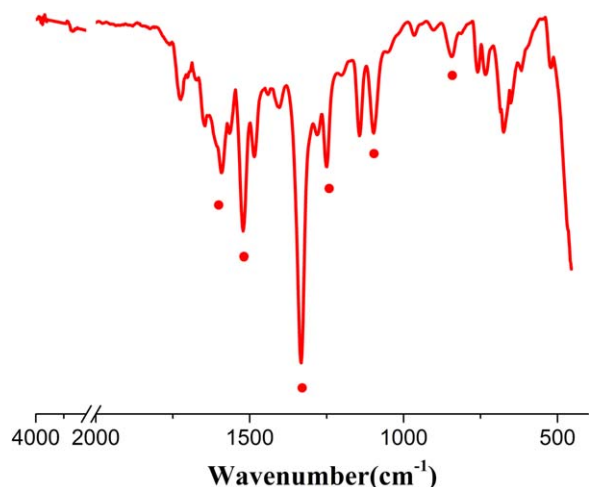


Figure 2. The FT-IR spectra of Fe-TNPc. [Color figure can be viewed in the online issue, which is available at wileyonlinelibrary.com.]

solvent. In this manner, three samples, with Fe-TNPc contents of 0, 0.5, and 1 wt %, were prepared; they were named Pc0, Pc0.5, and Pc1, respectively. Fe-TNPc had favorable compatibility with PU matrix as shown in Supporting Information Figure S1.

Characterization

¹H NMR Analysis. ¹H NMR spectra were obtained on an AVANCE/DMX 400 spectrometer (400 MHz, BUKER, Switzerland) in DMSO-*d*₆ solvent.

Tensile Tests. Tensile tests were performed on a universal material tensile machine (WDW3020, Changchun Greatwall Machine

Table II. The Solubility of Fe-TNPc^a

Solvent	DMSO	DMF	DMAc	Ethanol	Methanol	H ₂ O
Fe-TNPc	○	○	○	×	×	×

^a × : insoluble ○ : soluble

Co., Ltd.) at 20°C. The size of the samples was 60 mm × 2 mm × 0.08 mm. The initial length was set to be 30 mm, and the crosshead speed was 200 mm/min. The results were averaged by at least five measured data.

Dynamic Mechanical Analysis (DMA). DMA data were obtained by a TA Q800 dynamic mechanical analyzer. The size of samples was about 11.0 mm × 7.0 mm × 0.30 mm. The tests were carried out from -70°C to 190°C at a heating rate of 3°C/min with the frequency of 30 Hz and the vibration amplitude of 15 μm. The parameters such as storage modulus and tanδ as a function of temperature of the samples were obtained.

Infrared Analysis (IR). The tests were performed on a Nicolet 8700 infrared spectrophotometer and the spectra were recorded by averaging 64 scans at a resolution of 1 cm⁻¹. The films for infrared analysis were sufficient thin to be within the absorbance range where the Beer-Lambert law was obeyed.

Antibacterial Tests. The antibacterial activity was evaluated quantitatively using the shake flask method. *S. aureus*, a Gram-positive bacterium, and *E. coli*, a Gram-negative bacterium, which were commonly found on the human body, were chosen as the tested bacteria. The procedure was as follows: 1 ± 0.1 g of samples, cut into a size about 0.5 × 0.5 cm², were dipped

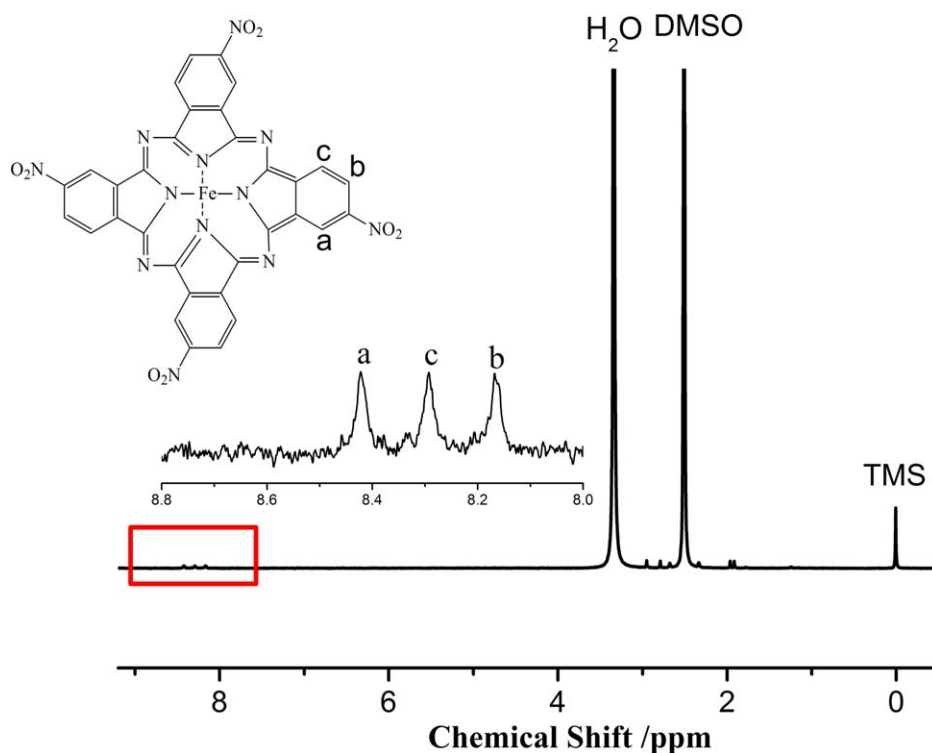


Figure 3. The ¹H NMR spectra of Fe-TNPc. [Color figure can be viewed in the online issue, which is available at wileyonlinelibrary.com.]

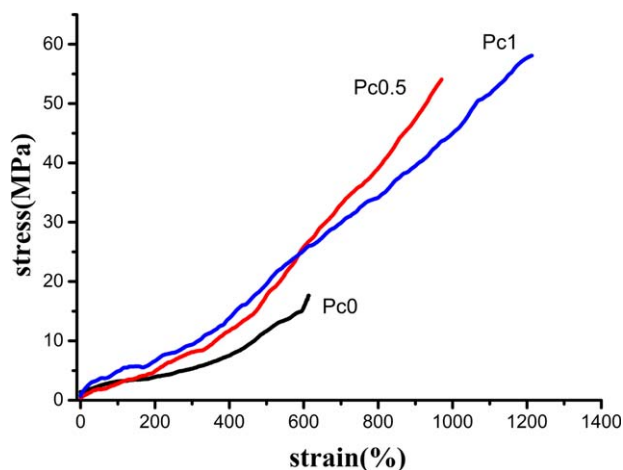


Figure 4. Strain–stress relations for PU and the blends. [Color figure can be viewed in the online issue, which is available at wileyonlinelibrary.com.]

into Erlenmeyer flasks containing 100 mL of fermentation medium with a cell concentration about $2 \times 10^5/\text{mL}$, respectively. The culture was shaken at 37°C for 24 hr under white light. One milliliter of the test solution was extracted after shaking, and then diluted and spread onto an agar plate. After incubation at 37°C for 24 hr, the number of colonies formed on the agar plate was counted and the number of live bacterial cells in the flasks after the shaking was calculated. Antimicrobial efficiency was determined based on duplicated test results.

RESULTS AND DISCUSSION

Preparation of Fe-TNPc

Fe-TNPc was synthesized according to the route as shown in Scheme 1. In order to obtain a higher yield of Fe-TNPc, the influence of the microwave power and the amount of catalyst on the yield of Fe-TNPc were investigated and shown in Figure 1. There was no generation of Fe-TNPc when the power of microwave was lower than 220 W. With the increase of microwave power, the yield of Fe-TNPc increased. At 295 W, it reached the maximum yield. The influence of the amount of catalyst on the yield of Fe-TNPc showed that the maximum yield was obtained when the amount of the catalyst was 0.2 mL. Thus, in this study, Fe-TNPc was synthesized under a 295 W irradiation with the amount of the catalyst to be 0.2 mL.

Characterization of Fe-TNPc

Figure 2 shows the Fourier transform infrared (FT-IR) spectra of Fe-TNPc. Peaks at 1332 and 1519 cm^{-1} corresponded to the symmetric and asymmetric stretching vibration bands of nitro-group. Peaks at 841 , 1096 , 1259 , and 1614 cm^{-1} corresponded

Table III. Mechanical Properties of PU and the Blends

Sample	Tensile strength (MPa)	Elongation at break (%)
Pc0	18.6	616
Pc0.5	52.6	952
Pc1	57.9	1206

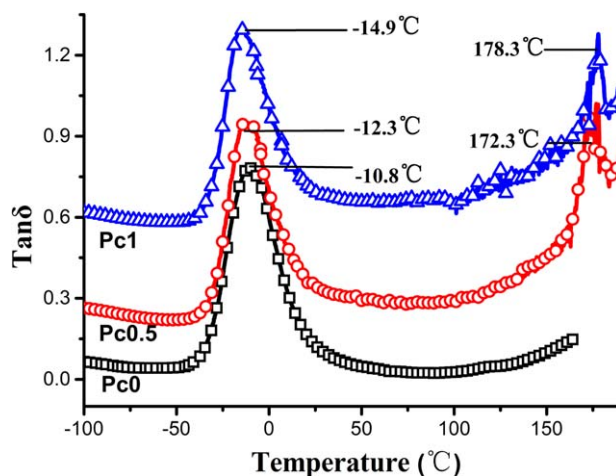


Figure 5. Temperature dependence of loss tangent ($\tan\delta$) for the samples (Pc0+0; Pc0.5+0.2; Pc1+0.5). [Color figure can be viewed in the online issue, which is available at wileyonlinelibrary.com.]

to the stretching vibration bands of Pc's skeleton. Figure 3 shows the $^1\text{H NMR}$ spectra of Fe-TNPc. The chemical shift values at 8.4, 8.3, and 8.2 corresponded to the three types of hydrogen atoms in Fe-TNPc. The related ratio of their integral area was 1 : 1 : 1, which indicated a successful synthesis of Fe-TNPc.

Table II shows the solubility of Fe-TNPc in solvents. It could be seen that Fe-TNPc had a good solubility in DMSO, DMF, and DMAc.

Characterizations of Fe-TNPc/PU Blends

Mechanical Properties. Figure 4 shows the stress-strain curves of Fe-TNPc/PU blends. The corresponding tensile strength and the elongation at break of the samples are listed in Table III. It showed that the tensile strength of the samples increased from 18.6 to 57.9 MPa and the elongation at break of the samples increased from 616% to 1206% with the increase of Fe-TNPc content from 0% to 1%. The incorporation of Fe-TNPc improved the mechanical properties of PU. It implied that Fe-TNPc might have a strong interaction with PU matrix. In order

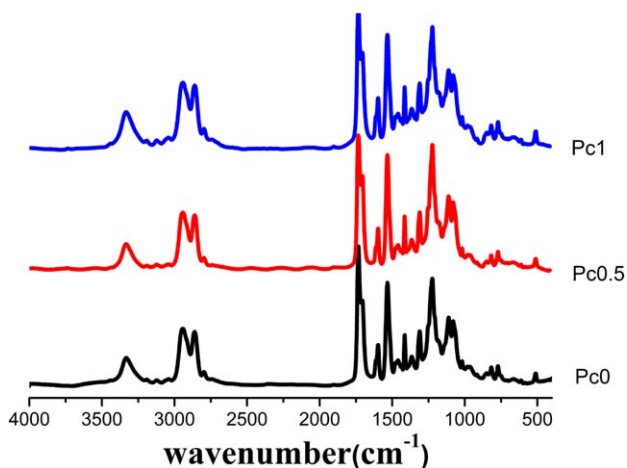


Figure 6. Infrared spectra of the samples. [Color figure can be viewed in the online issue, which is available at wileyonlinelibrary.com.]

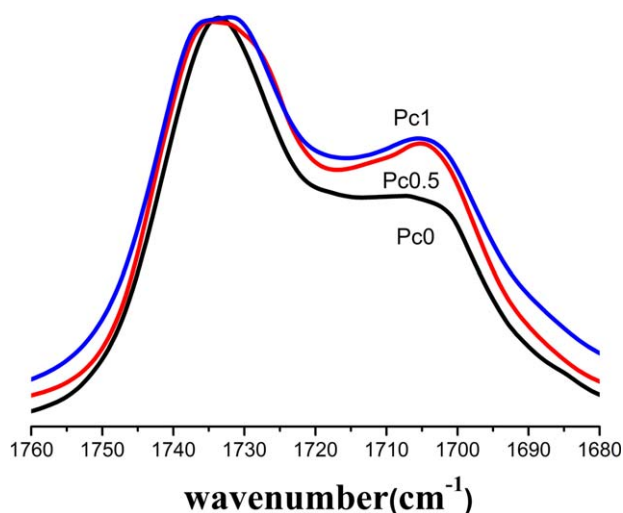


Figure 7. Infrared spectra of the carbonyl stretching of the samples. [Color figure can be viewed in the online issue, which is available at wileyonlinelibrary.com.]

to investigate the interaction between Fe-TNPc and PU matrix, DMA of the samples were studied.

Dynamic Mechanical Analysis. Figure 5 displays the curves of $\tan\delta$ as a function of temperature of the samples. The glass transition temperature (T_g) of PU can be characterized as the temperature associated with the peak magnitude of $\tan\delta$. From Figure 5 all the samples show a loss peak around -12°C , which corresponds to T_g of the soft segments of PU. It could be found that T_g of the soft segments of the samples shifted to lower temperature by incorporating Fe-TNPc, which indicated that the T_g value tended more closely to that of the pure soft segment. On the other hand, at the high temperature region, an obvious irreversible deformation of Pc0 was occurred when the temperature was above 160°C , which stopped the test process. T_g of the hard segments of Pc0 could not be obtained.¹⁸ But the

value of $\tan\delta$ increased when the temperature exceeded 160°C . The trend implied that T_g of the hard segments of Pc0 might be at a higher temperature than 160°C . For Pc0.5 and Pc1, peaks at 172.3°C and 178.3°C were showed up, respectively. The temperatures for the peaks might correspond to T_g of the hard segments of Pc0.5 and Pc1. It indicated that T_g of the hard segments of the samples increased with increasing Fe-TNPc content. The lower T_g of the soft segments and the higher T_g of the hard segments for the samples containing Fe-TNPc indicated that the microphase separation degree of PU increased with increasing Fe-TNPc content.^{18,25–30}

Infrared Analysis. Figure 6 shows the infrared spectra of the samples. The absorption peaks at $3210\text{--}3460\text{ cm}^{-1}$ and $1680\text{--}1760\text{ cm}^{-1}$ corresponded to --NH stretching vibration and carbonyl stretching vibration of PU, respectively.^{31,32} It was shown that the three IR spectra were almost the same. However, differences were showed up when we magnified the carbonyl stretching region, which could reflect the hard-hard segments hydrogen bond of PU, namely hydrogen bonded carbonyls ($\text{NH}\cdots\text{O}=\text{C}$ bond) of PU,^{33–36} as shown in Figure 7. Peaks centered near 1734 cm^{-1} and 1706 cm^{-1} were assigned to the stretching of free and hydrogen bonded carbonyl groups, respectively. The peaks around 1706 cm^{-1} became sharp. It indicated that with the incorporation of Fe-TNPc, the fraction of hydrogen bonded carbonyl groups of PU increased. More detailed information was obtained when curve fitting procedure^{31,37} was introduced. The results are shown in Figure 8. With the curve fitting procedure, the carbonyl stretching region of the spectra for the samples could be curve fitted by two Gaussian bands, corresponding to free and hydrogen bonded carbonyl band centered near 1734 cm^{-1} and 1706 cm^{-1} , respectively. X_b is defined as the fraction of hydrogen bonded carbonyl and can be expressed by the following equation:

$$X_b = A_b / (A_b + A_f), \quad (1)$$

where A_f and A_b is the area of free and hydrogen bonded carbonyl band, respectively.

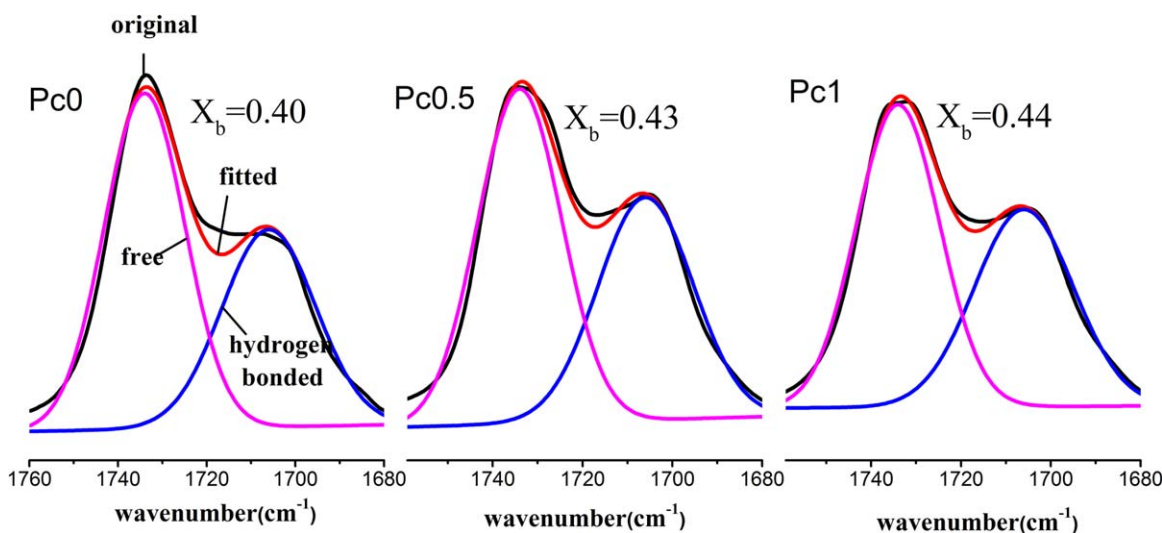


Figure 8. Curve-fitting results in the carbonyl stretching region of the samples. [Color figure can be viewed in the online issue, which is available at wileyonlinelibrary.com.]

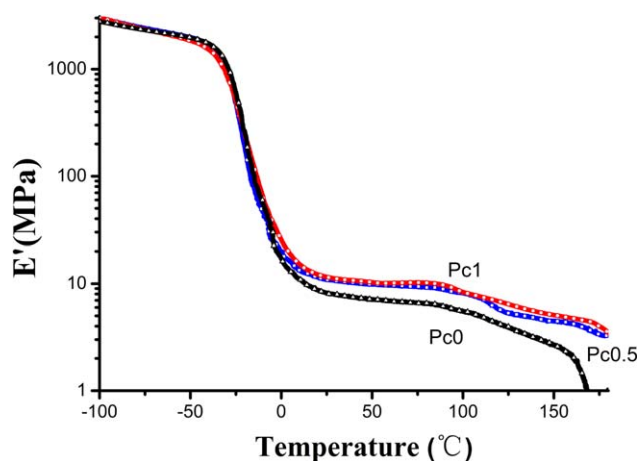


Figure 9. Temperature dependence of storage modulus (E') for the samples. [Color figure can be viewed in the online issue, which is available at wileyonlinelibrary.com.]

The results showed that the fraction of hydrogen bonded carbonyl of Pc0, Pc0.5, and Pc1 were 0.40, 0.43, and 0.44. It demonstrated that with the increase of Fe-TNPc content, the fraction of hydrogen bonded carbonyl increased. Fe-TNPc facilitated the formation of hydrogen bonded carbonyl groups of PU. The separated hard segments which dispersed in the soft segments of PU were aggregated by the incorporation of Fe-TNPc. As a result, the hard and soft segments of PU were more likely to separate from each other. Thus, the degree of microphase separation of the samples containing Fe-TNPc increased. The result was consistent with the results obtained from DMA and tensile tests.

Quantitative Evaluations of the Interaction Between Fe-TNPc and PU. It is well known that TPU is physically crosslinked. The physical crosslinks in PU are mainly arisen from hydrogen bond between the hard segments of PU. Therefore, the change of physical crosslinking density (v_s/V) in the samples could also be used to characterize the change of hydrogen bond of the hard segments of the samples. The storage modulus (E') versus

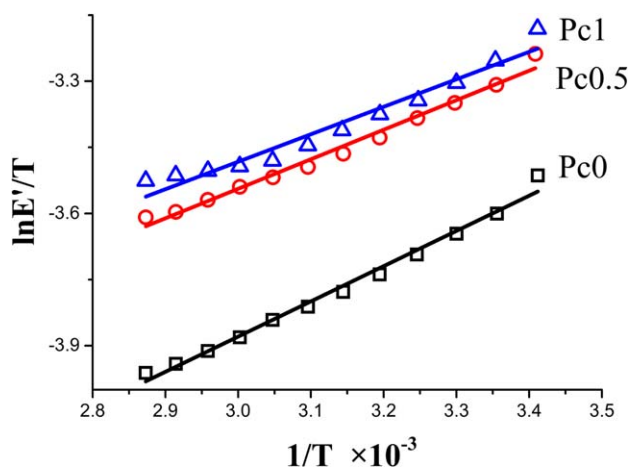


Figure 10. Plots of $\ln(E'/T)$ versus $1/T$ for the samples. [Color figure can be viewed in the online issue, which is available at wileyonlinelibrary.com.]

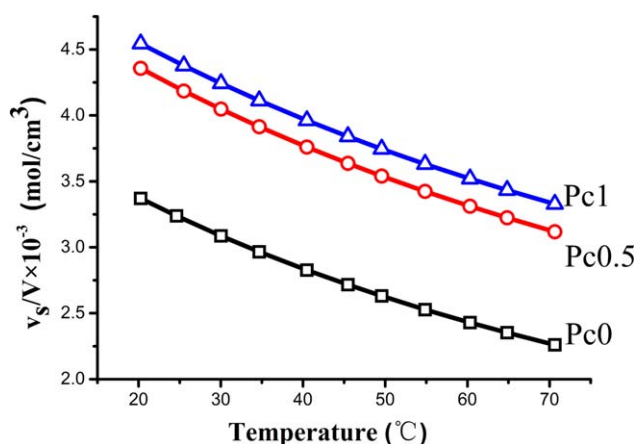


Figure 11. Effect of the temperature and the content of Fe-TNPc on the physical crosslinking density (v_s/V) of the samples. [Color figure can be viewed in the online issue, which is available at wileyonlinelibrary.com.]

temperature for the Fe-TNPc/PU blends are shown in Figure 9. At the low temperature where the samples were in the glassy state, the values of E' of the samples were almost the same. At the temperature above T_g of the soft segments, the values of E' increased with increasing Fe-TNPc content. All the samples showed a broad plateau modulus between 20°C and 80°C. The physical crosslinks in PU might be dissociated with increasing temperature. As a result, the rubbery plateau modulus of PU decreased with increasing temperature. The increased plateau modulus with increasing Fe-TNPc content indicated that the physical crosslinks in PU increased with increasing Fe-TNPc content.

v_s/V of the samples, which could be estimated by the value of E' at the rubbery plateau, as a function of temperature was studied in this article. The plateau modulus of the samples from 20°C to 80°C was used. v_s/V was calculated by using the same method in our previous paper.¹⁸

For an elastomer, the measured storage modulus can be expressed as:

$$E' = (v_s/V)RT. \quad (2)$$

According to Weisfeld et al.³⁸, v_s/V can be expressed by the Arrhenius relationship:

$$v_s/V = A \exp(E_a/RT), \quad (3)$$

where A stands for a constant, R is the gas constant, T is the absolute temperature, and E_a is the activation energy of hydrogen bond dissociation.

Using eqs. (2) and (3), we can obtain:

$$\ln(E'/T) = \ln(AR) + E_a/(RT), \quad (4)$$

E_a and A can be obtained from the slope and intersection of the straight line by plotting of $\ln(E'/T)$ versus $1/T$, as shown in Figure 10. Thus, v_s/V can be calculated by eq. (3).

The effect of the content of Fe-TNPc on the temperature dependence of v_s/V is shown in Figure 11. The values of v_s/V increased with increasing Fe-TNPc content. It indicated that the incorporation of Fe-TNPc increased the physical crosslinking

Table IV. The Percentage Bacterial Reduction of the Samples Toward *S. aureus* and *E. coli*

Sample	<i>S. aureus</i> reduction (%)	<i>E. coli</i> reduction (%)
Pc0.5	98.8	87.4
Pc1	98.9	90.9

density of PU, which was consistent with the conclusions above. The microphase separation degree of PU increased with increasing Fe-TNPc content.

Antibacterial Properties. The antibacterial mechanism of Pc has been widely investigated.^{39–43} With the irradiation of light, Pc can produce singlet oxygen to kill bacteria. The singlet oxygen can react with intercellular molecules (peptides and proteins, etc.) leading to oxidative damage of the cell wall and cell membrane.

The percentage bacterial reduction for the samples against pure PU was calculated according to the following eq. (5):

$$R = (B - A) / B \times 100\%, \quad (5)$$

where R is the percentage bacterial reduction, A is the number of live bacterial cells in the flask with Pc1 or Pc5 after shaking, B is the number of live bacterial cells in the flask with Pc0 after shaking.

The percentage bacterial reduction of the samples toward *S. aureus* and *E. coli* are shown in Table IV. The percentage bacterial reduction toward *S. aureus* for Pc0.5 and Pc1 was 98.8% and 98.9%, while the percentage bacterial reduction toward *E. coli* for Pc0.5 and Pc1 was 87.4% and 90.9%. Compared with Fe-OCAP/PU blends,²⁰ where Fe-OCAP/PU blends showed 96% bacterial reduction toward *S. aureus* when 5% Fe-OCAP was added into PU, Fe-TNPc/PU blends showed a higher efficiency toward bacterial inactivation. The modified samples had a high activity toward bacterial inactivation for both Gram-positive bacteria and Gram-negative bacteria and may have a potential industrial application in antibacterial fibers, coatings, etc.

CONCLUSION

In this article, Fe-Tetranitro phthalocyanine (Fe-TNPc)/polyurethane (PU) blends were prepared by solution blending. With increasing Fe-TNPc content, the tensile strength and the elongation at break of the samples increased. The improved mechanical properties for the samples containing Fe-TNPc were attributed to the increased microphase separation degree of PU with increasing Fe-TNPc content. The lower T_g of the soft segments and the higher T_g of the hard segments for the samples containing Fe-TNPc indicated an increase of microphase separation degree of PU. The increased hydrogen bonded carbonyl groups in the samples with increasing Fe-TNPc content also proved the conclusion. Quantitative evaluation of the interaction between Fe-TNPc and PU indicated that the physical cross-linking density of the samples increased with increasing Fe-TNPc content. The antibacterial tests showed that with increasing Fe-TNPc content the samples showed increased bacterial inactivation toward *S. aureus* and *E. coli*.

ACKNOWLEDGMENTS

This work was supported by the Program of Introducing Talents of Discipline to Universities (No. 111-2-04) and Chinese Universities Scientific Fund (CUSF-DH-D-2013006).

REFERENCES

- Feng, F.; Ye, L. *J. Appl. Polym. Sci.* **2010**, *119*, 2778.
- Kojio, K.; Mitsui, Y.; Furukawa, M. *Polymer* **2009**, *50*, 3693.
- Gireesh, K. B.; Jena, K. K.; Allauddin, S.; Radhika, K. R.; Narayan, R.; Raju, K. V. S. N. *Prog. Org. Coat.* **2010**, *68*, 165.
- Lee, H. T.; Lin, L. H. *Macromolecules* **2006**, *39*, 6133.
- Jang, E. S.; Khan, S. B.; Seo, J.; Nam, Y. H.; Choi, W. J.; Akhtar, K.; Han, H. *Prog. Org. Coat.* **2011**, *71*, 36.
- El-Sayed, A. H. M. M.; Mahmoud, W. M.; Davis, E. M.; Coughlin, R. W. *Int. Biodeter. Biodegr.* **1996**, *37*, 69.
- Dutta, S.; Karak, N.; Saikia, J. P.; Konwar, B. K. *J. Polym. Environ.* **2010**, *18*, 167.
- Das, B.; Chattopadhyay, P.; Mishra, D.; Maiti, T. K.; Maji, S.; Narayan, R.; Karak, N. *J. Mater. Chem. B* **2013**, *1*, 4115.
- Liu, H.; Dai, S. A.; Fu, K.; Hsu, S. *Int. J. Nanomed.* **2010**, *5*, 1017.
- Ma, X.; Zhang, W. *Polym. Degr. Stab.* **2009**, *94*, 1103.
- Akbarian, M.; Olya, M. E.; Ataefard, M.; Mahdavian, M. *Prog. Org. Coat.* **2012**, *75*, 344.
- Hsu, S.; Tseng, H.; Lin, Y. *Biomaterials* **2010**, *31*, 6796.
- Cho, D. L.; Chol, C. N.; Kim, H. J.; Kim, A. K.; Go, J. *J. Appl. Polym. Sci.* **2001**, *82*, 839.
- Masilela, N.; Kleyi, P.; Tshentu, Z.; Priniotakis, G.; Westbroek, P.; Nyokong, T. *Dyes Pigments* **2013**, *96*, 500.
- Hashimoto, K.; Toukai, N. *J. Mol. Catal. A* **2003**, *195*, 275.
- Meng, F.; Zhao, R.; Xu, M.; Zhan, Y.; Lei, Y.; Zhong, J.; Liu, X. *Colloid Surface A* **2011**, *375*, 245.
- Meng, F.; Zhao, R.; Xu, M.; Zhan, Y.; Lei, Y.; Zhong, J.; Liu, X. *Appl. Surf. Sci.* **2011**, *257*, 5000.
- Ti, Y.; Chen, D. *Prog. Org. Coat.* **2012**, *76*, 119.
- Ti, Y.; Chen, D. *J. Appl. Polym. Sci.* **2013**, *130*, 2265.
- Ti, Y.; Wu, J.; Chen, D. *Adv. Mater. Res.* **2013**, *750-752*, 1609.
- Lunardi, C. N.; Rotta, J. C. G.; Tedesco, A. C. *J. Porphyrins Phthalocyanines* **2003**, *7*, 493.
- Liu, M. O.; Hu, A. T.; *J. Organomet. Chem.* **2004**, *689*, 2450.
- Lokesh, K. S.; Uma, N.; Achar, B. N.; *Polyhedron* **2009**, *28*, 1022.
- Liu, M. O.; Tai, C.; Wang, W.; Chen, J.; Hu, A. T.; Wei, T. *J. Organomet. Chem.* **2004**, *689*, 1078.
- Kojio, K.; Mitsui, Y.; Furukawa, M. *Polymer* **2009**, *50*, 3693.
- Seymour, R. W.; Cooper, S. L. *Macromolecules* **1973**, *6*, 48.
- Adsuar, M. S.; Blas, M. M.; Martínez, J. M.; Villenave, J. *Int. J. Adhes. Adhes.* **1997**, *17*, 155.
- Lee, H. S.; Wang, Y. K.; Hsu, S. L. *Macromolecules* **1987**, *20*, 2089.

29. Lu, Y.; Tighzert, L.; Dole, P. Erre, D. *Polymer* **2005**, *46*, 9863.
30. Kojio, K.; Mitsui, Y.; Furukawa, M. *Polymer* **2009**, *50*, 3693.
31. Teo, L.S.; Chen, C.Y.; Kuo, J.F. *Macromolecules* **1997**, *30*, 1793.
32. Seymour, R. W.; Cooper, S. L. *Macromolecules* **1973**, *6*, 48.
33. Cleveland, C. S.; Guigley, K. S.; Painter, P. C.; Coleman, M. M. *Macromolecules* **2000**, *33*, 4278.
34. Mattia, J.; Painter, P. *Macromolecules* **2007**, *40*, 1546.
35. Chen, S.; Hu, J.; Zhuo, H.; Yuen, C.; Chan, L. *Polymer* **2010**, *51*, 240.
36. Brunette, C. M.; Hsu, S. L.; MacKnight, W. J. *Macromolecules* **1982**, *15*, 71.
37. Coleman, M. M.; Lee, K. H.; Skrovanek, D. J.; Painter, P. C. *Macromolecules* **1986**, *19*, 2149.
38. Segalla, A.; Borsarelli, C. D.; Braslavsky, S. E.; Spikes, J. D.; Roncucci, G.; Dei, D.; Chiti, G.; Jori, G.; Reddi, E. *Photochem. Photobiol. Sci.* **2002**, *1*, 641.
39. Moinuddin khan, M. H.; Venugopala Reddy, K. R.; Keshavayya, J. *J. Coord. Chem.* **2009**, *62*, 854.
40. Mosinger, J.; Jirsák, O.; Kubát, P.; Lang, K.; Mosinger, B. *J. Mater. Chem.* **2007**, *17*, 164.
41. Pereira, J. B.; Carvalho, E. F. A.; Faustino, M. A. E.; Fernandes, R.; Neves, M. G. P. M. S.; Cavaleiro, J. A. S.; Gomes, N. C. M.; Cunha, A.; Almeida, A.; Tomé, J. P. C. *Photochem. Photobiol.* **2012**, *88*, 537.
42. Mori, G. D.; Fu, Z.; Viola, E.; Cai, X.; Ercolani, C.; Donzello, M. P.; Kadish, K. M. *Inorg. Chem.* **2011**, *50*, 8225.
43. Weisfeld, L. B.; Little, J. R.; Wolstenbolme, W. E. *J. Polym. Sci.* **1962**, *56*, 455.